Foam injection applied to SAGD for improving thermal efficiency in presence of thief zones

A. PEREZ-PEREZ, A. M. KAMP (now with TOTAL)
CHLOE, UFR Science, University of Pau, BP 1155, 64013 Pau cedex, France

V. THEBAULT, G. DARCHE (now with TOTAL EP Congo)
TOTAL, CSTJF, 64000, Pau, France

Abstract

The importance of heat losses to cap rock during steam injection is known since the invention of steam flooding. A solution is to inject a non-condensable gas, either with the steam, or through a separate injection well. If the gas is lighter than the water vapor, it will rise through buoyancy to the top of the steam zone, where it will generate an insulating layer. The inconvenient is that the mobility of this gas is very high, so only slight pressure gradients are sufficient to make it move. If a thief zone (aquifer or gas cap) is located above the oil reservoir and there is not a sealing barrier, gas can escape from the reservoir reducing its insulating capacity.

This paper reports some numerical results of on-going research to reduce heat losses to a thief zone by using foam in a heavy oil reservoir produced by the SAGD process. We show a well configuration that permits injecting foam close to the bottom of the thief zone. The foam insulates the steam chamber from the thief zone which reduces the heat losses to the overburden. As a result, the thermal efficiency of the process increases and more oil is produced per volume of injected steam.

In this work, we show results of this application for Canadian reservoir conditions. A simplified lamella foam model was used based on literature results for forecasting foam behavior during steam injection. In the numerical model, gas mobility is reduced through a modified gas relative permeability and a viscosity function which depend on lamella molar fraction in the gas phase. The foam model includes pseudo-chemical reactions for generation and coalescence of lamellae, thermal degradation and surfactant adsorption on rocks.

For comparing numerical results, we select first the SAGD base line case with different injection strategies. The effect of co-injection of steam and methane was also evaluated. Then we compare best numerical results vs. the SAGD configuration plus foam injection at the top of the reservoir. Results show that the foam injection with a second injector well is able to reduce the heat losses to thief zones and also reduces the cumulative steam-oil ratio during the SAGD process. The effect of gas mobility reduction factor and foam decay at high oil saturation in the control of heat losses to the thief zone was also studied. Simulations show that results are very sensitive to these parameters which suggest the importance of measuring them at steam injection conditions during a controlled lab experience.

Introduction

The effect of the presence of gas cap and top water on SAGD performance has been well studied during the last two decades. In general, as the steam chamber came into contact with an overlying thief zone, heat was diverted away from the oil zone into the water zone, leading to the formation of condensate. The steam injected is not capable to provide enough latent heat to maintain the steam chamber, and consequently, recovery is severely affected. As it is reasonably expected, it is desirable to retain as much heat in the reservoir as possible. The presence of a top gas zone and mobile water cap has been reported on some specific Canadian reservoirs (Nasr *et al*, 2000a; Bao *et al*, 2010). Law and Nasr from the ARC were the first to investigate experimentally (2000a) and numerically (2000b) the SAGD process in the presence of a thief zone. Two experiments, the first with a non-confined water zone overlying the oil zone, and the second with a non-confined gas cap overlying the oil

zone, were conducted at field conditions to mimic SAGD in the Athabasca region. They observed that steam moves into both the top water and gas cap, however, more penetration of steam into the top water zone than in the gas cap was observed. Only 7 percent of additional oil was recovered after steam penetrated the top water zone. Oil was also displaced to the thief zones with percentages that vary from 10% OOIP into the water zone to 16% OOIP into the gas cap. Field scale numerical simulations from Law et al (2000c) based on lab experiments showed that operating conditions that lead to higher pressure difference between the steam chamber and the top water, either by depletion of the top thief zone or by increase on steam injection pressure, results in a detrimental effect on the SAGD performance. They obtained from simulation results that cumulative steam-to-oil ratio doubled when results from a non-confined top water zone were compared to a base line case of SAGD without top water.

The classical strategy of SAGD optimization in presence of a top thief zone is starting with a high injection pressure in the SAGD pair to promote vertical steam chamber grow. Once steam reaches the oil-pay top, the injection pressure is reduced to balance pressures between both zones with the intention to reduce heat losses to overburden and to promote lateral steam chamber spread. Even if CSOR is maintained low using this strategy, in general, oil production decreases significantly when reducing steam injection pressure affecting the economy of the SAGD process.

Gates et al (2007) did some simulations in a reservoir with a top gas zone, following this optimized steam-injection strategy and they verified that this promotes heat transfer in the lateral direction over that in the vertical direction. In the same direction, Gates and Chakrabarty (2006) studied the optimization of SAGD in presence of a mobile water cap for a McMurray reservoir section. They proposed a genetic algorithm to minimize a cost function based on cSOR in a heterogeneous 2D reservoir. They found an optimal cSOR around of 3.5 m^3 CWE (cold water equivalent) per m^3 oil at SC after six years of operation. They started the exploitation at initial injection pressure (2000 kPa) higher than reservoir pressure (1670 kPa) for one year and then the steam injection was followed by a stepped reduction in injection pressure until 400 kPa for five years. One of the problems of the reservoir model used by Gates and Chakrabarty is that a confined water cap was used, permitting the pressurization and heating of the thief zone which promotes the accumulation of heat in the aquifer and the increment of the temperature in the thief zone. On the contrary, the employment of a non-confined water cap in the numerical model infers the presence of at semi-infinite thief zone able to produce probably more realistic but less optimistic results if the thief zone is large enough beyond the reservoir model boundaries. Alturki et al (2010) examines the feasibility of SAGD operating strategies with a non-confined top water zone. They evaluated different strategies from overbalanced, balanced, underbalanced injection, stepped decline injection pressure and co-injection of methane (2% of mole fraction) with steam. The optimal strategy that prevents the steam chamber from collapsing to the top water zone, managing injection pressure (slightly over balanced or slightly under balanced), generated oil recovery factor of around 30 % OOIP and "optimized" cSOR of around 12 m^3 CWE/m^3 oil at SC after eight years of steam injection.

Bao et al (2010) using a 3D geostatistical model for the Surmont pilot (three SAGD pairs on Surmont lease, Athabasca) did a sensitive study using CMOST and STARS from CMG with the purpose of doing a history matching. They investigated the impact of a combined thief zone taking in to account a water cap (10 m) and a gas cap (4 m). They studied thief zones sensitivities varying the relative position of the top gas and water zones with respect to the pay zone. They concluded that a case with only top gas over bitumen is worse in term of oil production and cSOR than the case having both top water and top gas above it. In general, cSOR was around 8-10 m^3 CWE/m^3 oil produced at SC for three SAGD pairs after ten years of step-wise injection pressure from 2500 to 1000 kPa.

The injection of non-condensable gases (NCG) is another alternative that has been tested to control heat losses. In this process, a high concentration of non-condensable gases accumulates in the steam chamber, particularly near the top, resulting in a lower temperature at the top and providing a thermal cushion to reduce heat losses to overburden (Butler, 1999). One of the major concerns with NCG injection is that gases can impede the growth of the steam chamber due to convective heat exchange between steam and NCG (Butler, 2004; Ito et al, 2001). In addition, the leakage of this gas into the reservoir formation limits its isolation capacity to only a short period of time.

Low oil recovery factors and high values of cSOR found under optimal operation strategies and the limiting isolating capacity of NCGs have forced the research community to explore new alternatives to produce these reservoirs in a more efficient manner. The in situ formation of a diversion agent could be an alternative solution for reservoir that needs mobility control in presence of a thief zone on top. The benefits of injecting a diversion agent is to limit heat losses to the reservoir top that causes a reduction in the steam quantity injected per oil produced. In general, the injection of a diversion agent below the thief zone can promote the lateral extension of the steam chamber around the SAGD pair.

Foam and steam injection

The benefit of employing foam for diverting steam in thermal EOR process has been demonstrated in different field tests (Patzek, 1996). According to field projects, combination of foam plus steam had help to improve areal sweep, to improve steam distribution and to block thief zone. Foam had been also useful to improve heat accumulation during steam soaks. In general, two approaches have been used with steam foam. The first one is to inject surfactant plus steam to displace oil during foam drive. The second approach is to use foam to improve the steam injection profile. In general, steam foam injection reduces significantly gas mobility in porous media. The first steam-foam project was done by Shell in the Kern River field (Patzek, 1996). They injected steam-foam to improve vertical sweep efficiency. Another steam foam diversion project was the Gregoire Lake in situ steam pilot (GLISP) conducted in Athabasca (Sander et al, 1991). The original purpose of this pilot was to inject steam at the bottom of the McMurray formation through horizontal fractures in three vertical producers. Due to the fact that induced fractures were not completely horizontal, a communication between the injector and upper low-oil saturation zone was established, generating a very poor oil

recovery during the first steam cycles. After detecting the cause of the problem, steam foam injection was suggested to avoid that steam over-rides the rich oil tar sands. Initial response to foam injection showed an increase in steam injection pressure and an increment of 100% with respect to final oil production obtained at the end of the second steam cycle. The steam-oil ratio reduced from 8 to 5.5 m³ CWE/m³ oil SC. In this case, it was demonstrated that foam can divert steam to the bottom oil rich sand, reducing effectively the steam injection into a thief zone (formation top). Surfactant and non-condensable gases were injected during fifteen months. The project was stopped one year later after stopping surfactant injection. A total oil recovery of 38% OOIP was obtained at the end of the application. A history matching of this steam-foam injection process was done using an empirical foam model in STARS (Lau et Coombe, 1994).

Chen *et al* (2010a) have studied how to improve SAGD with foam. They showed numerically that foam-assisted SAGD (FA-SAGD) can control steam mobility and can generate a more uniform steam distribution based on a simplified population balance approach for foam. This local-equilibrium foam model had been previously validated with experimental results (Chen *et al,* 2010b). One of the purposes of injecting steam and a small amount of surfactant in a SAGD pair is to generate strong foam in place in the high permeability region around the injector well that results in a more uniform steam chamber development. It is well known that foam stability is affected by high temperatures and high oil saturations. One of the weaknesses of the FA-SAGD configuration is that foam should be generated around the injector well where the temperature and oil saturation are elevated which causes degradation of foam. This implies that large quantities of surfactant must be injected to improve the foam generation rate. It is worth noting that thermal degradation of surfactant and/or foam was not explicitly specified in Chen's model. We think that the fact that foam is generated in situ around the SAGD injection well can also affect steam injectivity.

The purpose of this document is to show a novel well configuration able to improve SAGD thermal efficiency in presence of a non-confined thief zone located above the pay zone. The co-injection of surfactant solution and non-condensable gas below the thief zone form a barrier of gas-blocking foam that promotes the lateral growth of the steam chamber. This barrier prevents steam contacting the thief zone, promoting that more heat is kept in the pay zone which results in more oil produced per barrel of steam injected.

In this work a general overview of a lamella foam model is first presented. Then, we describe our lamella foam model based on data from the literature. Our numerical approach includes pseudo-chemical reactions for generation and coalescence of lamellae, thermal degradation and surfactant adsorption on rocks. In this foam model, gas mobility is reduced in presence of foam through a modified gas relative permeability function and a viscosity function, both depending on lamella molar fraction in the gas phase.

After presenting the synthetic reservoir used in the simulations, the novel well configuration is presented for Canadian reservoir conditions. In this pattern, we suggest to perforate a second injector well, vertical or horizontal, in the top of the pay zone and close to the bottom of the thief zone to inject chemical products able to generate foam in situ. We believe that the foam formation in a region swept by steam or with low oil saturation on the top of the reservoir offers a favorable condition for generation and sustainance of foam due to simultaneous presence of water and injected fluids: gas and surfactant. In addition, we do not expect to have large amount of oil around the injected region that promotes foam decay.

For comparing numerical results, we select first the SAGD base line case based on injection strategies commonly used in presence of a thief zone: over balance, underbalance, stepped declining pressure respect to thief zone pressure and managing injection pressure with steam-oil ratio (SOR) control. The best performance with respect to heat accumulated in the pay zone, recovery factor and cumulative steam-oil ratio at a fixed time was selected as a SAGD base line case. For studying the ability of non-condensable gases (NCG) to improve the SAGD thermal efficiency in presence of a thief zone, different injection strategies of NCG co-injection in a SAGD well were evaluated. Then we compare these numerical results vs. the SAGD configuration plus foam injector at the top of the reservoir. Later, we show results for foams with different levels of gas mobility reduction and we present the effect of including foam decay by oil presence in the numerical model. Finally, we show our final comments and draw some conclusions.

Foam models and approaches

Based on laboratory observations, a variety of theoretical models has been developed to model foam flow through porous media. These models rely on the fact that foam texture determines the strength and mobility of foam. In general, foam texture depends on pore structure, surfactant formulation, permeability, capillary pressure and flow rates, presence of oil, etc. The existing theoretical models range from empirical models (Marfoe and Kazemi, 1987; Islam and Farouq, 1990; Coombe et al, 1990; Chou, 1995), to models based on fractional flow theory: the fixed-Pc* model (Fisher et al, 1990; Rossen et al, 1991), to network models (Rossen and Gauglitz, 1990), and to population-balance models (Kovscek *et al*, 1994; Chen *et al*, 2010). In this work, we show a description of the lamella density model which is an empirical model. This model is present in the commercial reservoir simulator STARS from CMG.

Empirical models

In general, empirical models deal with reduction of gas mobility in presence of foam by modifying either the relative permeability to gas, or viscosity of gas phase, or both. The following equation shows how gas mobility $\lambda_g{}^{foam}$ is modified in presence of foam

$$\lambda_g{}^{foam} = K \cdot \frac{K_{rg}^{foam}}{\mu_g{}^{foam}} \qquad (1)$$

The gas relative permeability with foam is defined as the product of the original gas relative permeability and a gas resistance factor, FM,

$$K_{rg}^{foam} = K_{rg} \cdot FM \qquad (2)$$

If the foam is very strong, the FM is very small and the relative permeability to gas with foam is smaller than the original gas relative permeability. On the contrary, if the foam is weak, the FM is around one and the relative permeability to gas with foam is close to the original gas relative permeability.

Lamella density model

This approach is based on the fact that foam is a non-equilibrium dispersion of surfactant-stabilized film of water which separates gas bubbles (Coombe *et al*, 1990). In this model, foam formation and foam destruction can occur at different time scales. This empirical approach consists in forming appropriate rate expressions for lamella generation, lamella coalescence and lamella capture and/or lamella adsorption to fit experimental results.

In the lamella foam model, a separated equation is introduced to account for conservation and transport of lamellae

$$-\nabla \cdot [\vec{u}_g \rho_g Y_l] + q_l + (r_{lg} + r_{lc} + r_{ld})$$
$$= \frac{\partial}{\partial t}(\varphi S_g \rho_g Y_l + (1-\varphi)Ad_l) \quad (3)$$

On the left side, the first term represents lamella convection in gas phase, the second is the source/sink term, and the third is the addition of the generation, coalescence, and decay rate of lamellae. On the right hand side, the first term and the second term of the time derivative denote the amount of lamella in gas phase and the pore blockage, respectively. Foam propagation will be stable if lamella generation rate is larger than the addition of lamella coalescence and decay rate. On the contrary, no foam will be formed if lamella generation rate is lower than the addition of lamella coalescence and decay rate.

It is expected that the trapped lamella reduce relative permeability to gas via a pore blocking mechanism. In this model, gas phase resistance factor, *FM* is defined as

$$FM = \frac{1}{1 + (RRF - 1) \cdot \frac{Ad_l}{Al_{max}}} \quad (4)$$

Additionally, the flowing lamellae are also expected to decrease gas phase mobility in equation (1), essentially due to an increase in gas phase viscosity. The gas viscosity is dependent on lamella molar fraction in gas phase and the pre-assigned viscosity for lamella component. The general equation of viscosity in presence of foam is given by

$$\mu_g^{foam} = \mu_g^o \cdot (1-Y_l) + \mu_l \cdot Y_l \quad (5)$$

Lamella density foam model requires many parameters that should be measured at lab conditions or obtained by history matching. The lamella density model was used in this work to assess different scenario of application of foam during steam injection.

1   Model description

In the following sub-sections, we describe the foam model and the synthetic reservoir model. The thermal reservoir simulator STARS from CMG was employed in this work.

1.1   Foam model

In the current work we have used model parameters from foam models described in literature (STARS Manual, 2011a-b). One model reproduces foam displacement experiments performed at high temperature by Friedmann *et al* (1987-1991). Other model represents a history matching performed for the steam-foam pilot test conducted in Gregoire Lake (Athabasca) reported by Lau and Coombe (1994).

In our model, foam or lamella are generated by the combination of a non-condensable gas (NCG) and a surfactant solution. NCG may be nitrogen, methane or any other NCG at the reservoir conditions. The foam model used in this work constitutes of five components. The components and phase distribution are shown in Table 1. The number in parenthesis is the molecular weight in g/gmole used in the simulation model.

In order to describe the formation and rupture of lamella, two reactions were specified in our foam model. In addition, a thermal degradation of surfactant was specified. In the kinetic model, reaction rates were directly proportional to the rate constant, K_i. The constant velocity follows Arrhenius temperature dependence composed by a pre-exponential factor A_i and activation energy, Eai.

$$K_i = A_i \exp - {}^{Eai}/_{RT} \quad (6)$$

The described chemical reactions and the reaction rate expressions are as follows

Lamella generation

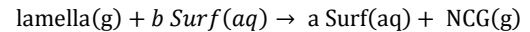$$a\ \text{Surf(aq)} + NCG(g) \rightarrow \text{lamella(g)} + b\ \text{Surf(aq)}$$
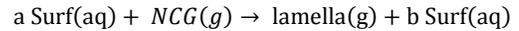
with a= 7.50E-02 and b=3.75E-02.
Reaction rate of lamella formation was expressed as

$$r_{lg} = (K_1)C_{Surf} \cdot C_{NCG} \quad (7)$$

Lamella coalescence

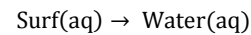$$\text{lamella(g)} + b\ Surf(aq) \rightarrow a\ \text{Surf(aq)} + NCG(g)$$

with reaction rate of lamella coalescence being

$$r_{lc} = -(K_2)C_{lamella} \cdot C_{Surf} \quad (8)$$

As described above, a stable regime of foam propagation is established when $r_{lg} \gg r_{lc}$. On the contrary, foam is not detectable if $r_{lg} \ll r_{lc}$.

Thermal degradation of surfactant

$$\text{Surf(aq)} \rightarrow \text{Water(aq)}$$

with reaction rate of surfactant degradation expressed as

$$r_{Surf} = -(K_3)C_{Surf} \quad (9)$$

The effect of including the thermal degradation of surfactant implies that lamella concentration depends also on temperature. The higher is the temperature, the lower is the amount of surfactant available to generate lamella according to equation (9).

Foam decay by oil presence

In addition, it is well known that foam stability can be altered by the presence of oil saturation. This effect is well documented in the literature (Jensen and Friedman, 1987; Hirasaki, 1989).The expression that can be used to model this phenomenon can be expressed as

$$\text{lamella}(g) + oil(o) \rightarrow \text{Surf}(aq) + \text{NCG}(g) + oil(o)$$
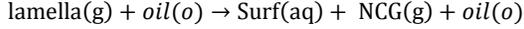
with foam decay rate being

$$r_{\text{Lamella}} = -(K_4)C_{\text{lamella}} \cdot C_{\text{oil}} \qquad (10)$$

It should be noticed that oil is present at both sides of equation. Oil is not consumed during foam decay. The higher the oil saturation, the larger the oil concentration ($C_{\text{oil}} = \varphi \cdot S_o \cdot \rho_o \cdot X_{oil}$) and in consequence, the larger the lamella degradation rate. Friedmann and Jensen (1987) have reported that large values of oil saturation can accelerate foam decay by 100 times.

Values for these kinetic expressions are summarized in Table 2. Data for lamella generation and coalescence were measured at isothermal conditions. On the contrary, surfactant decay shows dependence with temperature. Lamella decay as a function of temperature is not explicitly considered in our foam model due to the specification of surfactant thermal degradation. The effect of foam saturation on foam decay for the foam base case was not considered as a first approach. Later, we analyze the effect of foam decay in the foam model.

In the lamella density model, gas mobility is affected by the gas resistance factor, FM, and the apparent gas phase viscosity, μ_g^{foam}. Regrouping equation (2) and (5) in (1), foam mobility as a function of the original gas permeability and gas viscosity can be expressed as

$$\lambda_g{}^{foam} = K \cdot \frac{K_{rg}}{FF \cdot \mu_g^o} \qquad (11)$$

FF is the global gas mobility reduction factor in presence of foam. It is function of lamella effective viscosity, gas phase resistance factor and gas viscosity without lamella according to the following equation

$$FF = \frac{\mu_g^{foam}}{FM \cdot \mu_g^o} \qquad (12)$$

For the base foam model, we have decided to use a minimum global gas mobility reduction factor of 250. This implies that gas mobility in presence of the critical lamella concentration will not be lower than 250 times the value obtained when only gas is present. Gas mobility reductions of the order of 10 to 1000 have been reported at the literature for mobility control (Chen, 2009).

In order to simplify our lamella model the gas phase resistance factor, FM, was not considered as a function of lamella adsorption concentration as experimental data as a function of temperature are not available in the literature to

parameter this model. Therefore, a constant gas resistance factor once critical molar faction of lamella in the gas phase is reached was used in our current study. Using this procedure, we have reproduced steam-foam pilot test results from Gregoire Lake (Lau and Coombe, 1994). According to this assumption, gas relative permeability curves in presence of foam were divided by a constant. For the foam base case we have chosen a factor of 10, i.e., $FM = 1/10$, at specified critical lamella molar fraction in the gas phase. This critical lamella molar fraction is a value from which gas permeability reduction is taken into account. This implies that a reduction of ten times is expected in the original gas relative permeability when the critical lamella molar fraction is reached in the gas phase. In this foam model, we have defined a critical lamella molar fraction of 10^{-3}. If lamella molar fraction is lower than this critical value, no blocking is expected.

For completing the set of parameters used in the definition of the global gas mobility reduction factor, it is also necessary to describe the apparent foam viscosity. According to history matching of Friedman experiments performed by Coombe (STARS Manual, 2011a), lamella viscosity can have a value of 250 cP at steam injection condition. This implies that the apparent gas phase viscosity can go from $1 \cdot 10^{-2}$ to around $2.5 \cdot 10^{-1}$ cP when the critical lamella molar fraction is reached in the gas phase and there is no steam in gas phase. After combining foam viscosity and gas resistance factor we are able to obtain the desired minimum value of global gas mobility reduction factor (250) at the critical lamella molar fraction.

In the foam model, we was also included the surfactant adsorption as a function of temperature. The adsorption function as a function of temperature and surfactant concentration in water phase is shown in Figure 1. When temperature increases, surfactant is more soluble in water and less surfactant is available to be adsorbed on rock. No blockage (permeability or porosity reduction) was specified due to surfactant adsorption on rock.

1.2 Synthetic reservoir model

A synthetic reservoir representing a generic formation in Athabasca oil sand (western Canada) is described now. The reservoir consists of two sectors: a pay zone rich in oil and a thief zone above it. The pay zone was 50 m in length and 40 m in thickness. The thief zone located above it is 10 m high. Figure 2 shows a general description of the model.

For simulating the SAGD recovery process, a horizontal production well (P) with a length of 850 m was placed 1.5 m above the bottom of the pay zone. A horizontal injection well (I1) with the same length is situated parallel to the producer with a vertical well spacing of 5 m. The horizontal spacing between well pairs is 100 m. Due to symmetry and the assumption of a homogeneous system, we model only half of the unit. Our uniform 2D grid system contains 58 grid blocks in the x-direction and 50 grid blocks in the z-direction. The cells in the pay zone and thief zone are 50 m long. Grid cells were 1 m wide and 1 m high. To simulate a semi-infinite model, eight grid blocks with variable spacing were added to the model in the right side to complete 400 m. In addition, this permits to limit border effects around the pay zone. An injector of blocking agent, 'I2', was located 5 m below the thief zone. Well 'I2' is only open when foamer agents are

injected. In addition, a virtual sink 'P2', was located above the thief zone to keep thief zone pressure constant and equal to the original pressure during the whole oil recovery process. This well, which in reality does not exist, represents natural inflow of water in the thief zone. The reference initial pressure was 1000 kPa in the pay zone top.

Initial oil and water saturation in the pay zone were 0.8 and 0.2, respectively; while water saturation in thief zone was 1.0 (i.e. only water is present in the thief zone). Reservoir temperature was 10°C. The reservoir formation consist of clean sand, no heterogeneities were specified. The absolute permeability in the pay zone was 2000 mD in the horizontal direction while vertical permeability was 3/5 of the horizontal permeability. Porosity was 30%. Values of permeability and porosity for the thief zone were lower than for the pay zone, 1000 mD and 20%, respectively. Detailed reservoir properties are listed in Table 3.

A decreased function of oil viscosity as a function of temperature was used for a heavy Athabasca oil. Gas viscosity of components as a function of temperature was expressed as $8.3E-05 \cdot T^{0.9}$ (cP) with temperature in Kelvin.

Water-oil and gas-oil relative permeability curves as a function of lamella molar fraction in the gas phase were specified. Note that at critical lamella molar fraction in the gas phase, original gas relative permeability was multiplied by the defined gas resistance factor, FM.

Heat losses from and to over burden and under burden were specified. Heat losses and mass transfer from or to the thief zone was permitted.

2 Studied cases

In this section a description of the studied cases is shown. Firstly, SAGD base line case is selected from classical strategies performed in presence of a thief zone: over balance, underbalance, stepped decline pressure with respect to water cap pressure and a managed steam injector with steam-oil ratio control. Similar procedure was followed to select a prospective case of non-condensable gas co-injection in the SAGD injector well. Then, we describe our proposed configuration with a second foam injector at the top of the pay zone. In the following two sub-sections, models used for studying the effect of gas mobility reduction factor and the effect of oil saturation in foam decay are presented.

For all cases, a preheating period of three months was specified for the SAGD pair. A period of ten years of simulation was studied for comparing different cases.

2.1 SAGD base line case

Four strategies were studied for selecting the SAGD base line case in presence of a thief zone on top. Injection strategies are referred to the initial reservoir pressure at the top of pay zone (1000 kPa). In general, the steam injector is controlled in injection pressure and in steam injection rate. Injected steam quality was 80%. In the following points, we describe the injection strategies:

- Overbalance or high injection pressure on SAGD: maximum steam injection pressure (BHP max) of 2500 kPa (Tsat=226°C) and maximum injection rate (Qmax) of 400 m^3 at SC/day.

- Under balance or low injection pressure on SAGD: BHP max of 2500 kPa for two years and then 1000 kPa (Tsat=184°C) from third years. Qmax of 400 m^3 at SC/day.

- Stepped decline case on SAGD: BHP max of 2500 kPa during the first year. BHP max of 1750 kPa (Tsat=208°C) during the second year and maximum BHP of 1000 kPa from third years. At any time, Qmax was fixed to 400 m^3 at SC/day.

- Managed steam injection pressure with steam-oil ratio control on SAGD: BHP max of 2500 kPa during two years and then maximum BHP of 1000 kPa from third year. At any time, Qmax was 400 m^3 at SC/day. SAGD pair is controlled to keep instantaneous steam to oil ratio in a maximum value of injected water (CWE) per m^3 of oil at SC.

The best performance with respect to heat accumulated in the pay zone, recovery factor and cumulative steam-oil ratio after ten years was selected as a SAGD base line case.

2.2 Gas co-injection in SAGD well

The addition of a non-condensable gas (NCG) to injected steam was studied for comparison purposes. The objective of co-injecting methane is to evidence the potential capacity of NCG in controlling heat losses through thief zone and reducing cumulative steam-oil ratio. A NCG (methane) was injected along with steam in the SAGD injector at a fixed volumetric fraction of 50 % (vol/vol) at surface conditions and after one and a half years of SAGD starting. This represents a methane molar fraction of 0.1 % at standard condition. Others more diluted NCG co-injection were tested but without better performance than steam alone cases. In these simulations presented here, a maximum quantity of steam injected in the reservoir was similar to the cases when only steam was injected. The following injection strategies were studied:

- Methane co-injection in overbalanced SAGD: maximum steam injection pressure (BHP max) of 2500 kPa and maximum total fluid rate (Q max) of 400 m^3 at SC per day per injected fluid.

- Methane co-injection in under balanced SAGD: one and a half years of steam injection followed by NCG and steam co-injection. BHP max for the steam alone period was 2500 kPa, then for the co-injection period was 1000 kPa. Control in total fluid rates (water and water-NCG period) equal to 400 m^3 at SC per day per injected fluid.

- Methane co-injection in stepped declining strategy for SAGD: steam injection with BHP max of 2500 kPa during the first year. Co-injection with BHP max of 1750 kPa during the second year and maximum BHP of 1000 kPa from the third year. At any time, total injection rate maximum was 400 m^3 at SC per day per injected fluid.

- Methane co-injection on SAGD with managed injection pressure with steam-oil ratio control: BHP max of 2500 kPa for the steam injection period then maximum BHP of 1000 kPa during one and a half year. At any time, total fluid injection rate maximum was 400 m^3 at SC per day per injected fluid. SAGD pair is controlled to keep instantaneous steam to oil ratio in a minimum value of injected water (CWE) per m^3 of oil at SC.

2.3 Foam injection at reservoir top

In addition to the SAGD pair, a second injector well located five meters below the pay zone top was placed to inject the chemical formulation that permits foam formation. Water, surfactant and NCG are injected in the dedicated well to form foam on the reservoir top. Volumetric compositions of the injected fluids were: 4.9 % water, 0.1% surfactant and 95% gas. Foam is in essence a dispersed solution of surfactant in a gas phase. Figure 2 shows a description of the complete foam configuration. Steam in the SAGD injector is injected at maximum bottom hole pressure of 2500 kPa and maximum steam rate of 400 m^3 at SC/day. The SAGD pair is controlled to keep instantaneous steam to oil ratio at a minimum value of injected water (CWE) per m^3 of oil at SC. A preheating period of three months is performed in the second horizontal well. The foam injector is open one year after starting steam injection and is controlled at maximum pressure of 1000 kPa. Injection pressure is slightly larger than bottom hole pressure of the thief zone in order to promote foam invading progressively the water zone and expanding laterally around the foam injector well.

2.4 Effect of gas mobility reduction

Five foam formulations with different levels of blockage were run. The foam base case shown above had a minimum global gas mobility reduction factor of 250. Additional cases with different levels of blocking effect were run to evaluate the effect of gas mobility reduction. The following global gas mobility reduction factors (FF) were evaluated: 2500, 1250, 250, 25 and 1, altering gas relative permeability (maximum relative gas permeability at connate liquid, Krgcl). For the case where FF=1, gas was injected on the second well but not surfactant to avoid foam generation. It should be mentioned that these global gas mobility reduction factors are minimum blocking factors that may be found when critical lamella concentration would be reached. As lamella concentration may be higher than the critical value, effective gas viscosity may be larger according to equation (5) and higher blockage may be obtained locally. For all cases, the foam injector was controlled at maximum injection pressure of 1000 kPa and a maximum gas volume of 400 m^3 at SC per day. In addition, 5% of surfactant solution was also injected. The foam injector was open one year after starting steam injection. The SAGD pair injects steam at maximum bottom hole pressure of 2500 kPa for twenty-seven months after which pressure was reduced to 1000 KPa. Additional constraint for the injector well was a maximum steam rate of 400 m^3 at SC/day. Injection pressure in the SAGD pair and the second injector

was kept similar for all cases for comparative purposes. The SAGD pair is controlled to keep instantaneous steam to oil ratio at a minimum value of injected water (CWE) per m^3 of oil at SC.

2.5 Effect of oil saturation in foam decay rate

The effect of oil saturation on foam stability was also studied in this work. We have considered two cases with different initial oil saturation in the thief zone: So=0 (foam reference case) and So=0.20. In this work, we have employed a foam decay measurement in presence of oil (So=0.20) reported by Friedmann and Jensen (1987) at 150°C and reported in the STARS manual (2011b). We have included equation 10 that permits to describe foam destruction when oil is present. According to this equation, reaction rate is first order with respect to oil and lamella concentration in the gas phase and K4 equals to 2.2 m^3/gmole day^{-1}. The foam injector and the SAGD pair were controlled the same way as in the foam base case, but gas rate was permitted to be higher (1000 m^3 at SC/day) in order to magnify the effect of foam decay in presence of oil.

3 Results and discussion

3.1 SAGD base line case

Results for different SAGD strategies to control steam injection in presence of a thief zone are summarized in Table 4. A cumulative injected steam column was also added. Twice the volume of water was injected in the overbalance case compared to the pressure reduction strategies or the steam-oil ratio control. In general, results showed that reducing steam injection pressure before the steam chamber contacts the thief zone can improve general SAGD performance. We have selected the stepped decline strategy as a SAGD base case for comparison purpose.

3.2 Gas co-injection in SAGD well

Figure 6 shows temperature and NCG molar fraction in the gas phase after 5 years of simulation in a reduced reservoir section of 50 meter length and 50 meter height. In this case, a 10 meter NCG cap acts as isolation between the steam and the thief zone. On the other hand, the presence of gas on top of the steam chamber causes its lateral expansion. This can promote more fresh oil being contacted by steam, improving eventually the oil recovery factor.

Table 5 summarized results for these cases after ten years of numerical simulation. In general, better results are obtained with gas co-injection strategies than when steam alone is injected with a reduction in injection pressure. Optimal steam gas co-injection results were obtained using the stepped decline strategy. This strategy gives the lowest CSOR and largest fraction of injected heat retained in the pay zone.

Table 5 also shows the total cumulative volume of water and gas injected in ten years. Volume of water is slighter larger than the gas volume due to a starting period of 1.5 years

without gas injection. The stepped decline case with gas co-injection gives lower volumes of water and gas for the largest values of oil recovery. When comparing Table 4 and Table 5, the stepped decline gas co-injection strategy gives lower values of cumulative steam-oil ratio for less volume of water injected.

Figure 4 compares steam chamber shape and NCG gas molar fraction in gas phase for two NCG co-injection cases: one, managing injection pressure to keep a minimum steam-oil ratio (SOR control) and two, stepped decline gas co-injection strategy. In the first strategy, gas was co-injected with steam after one and half year of steam alone, while for the second case, gas was co-injected after only one year of steam injection. The fact that gas would be co-injected in an early stage permits to inject more gas. In fact, 50% more gas volume was injected in the stepped decline strategy than in the other strategy for the time shown in the figure. This permits to create a gas cap thick enough (8-10 m) to limit vertical expansion of the steam chamber. For the case where only 3-5 m gas cap thickness was formed, no major resistance was obtained according to the steam chamber shape.

According to these results, it seems more convenient to follow a pressure reduction strategy during SAGD exploitation *accompanied with* an early NCG co-injection in the SAGD well. The fact that gas would be co-injected during the first step of the injection permits to place enough gas volume around the steam chamber. If the gas cap is thick enough gas can delay contact time between steam and water. This causes a lateral expansion of the steam chamber which is beneficial in presence of an upper thief zone.

If gas co-injection results are compared to SAGD base line results, NCG-steam co-injection strategy permits to reduce CSOR from 7.4 to 4.4 when a progressive pressure reduction strategy is adopted. For other strategies, under balance and instantaneous steam-oil ratio control, differences are negligible.

3.3   Foam injection in the reservoir top

In our proposed strategy to improve exploitation of SAGD configuration in presence of a top thief zone, foam is injected after one year of steam injection to limit contact between steam and water. Figure 5 shows the way lamellae are formed around the second horizontal well, together with its effect on gas mobility after five years of steam injection and four years of chemical injection in the second well. As it is clearly shown in the figure, lamella molar fraction in the gas phase varies from 1E-03 to 1E-01 and gas permeability is low in the thief zone where foam has penetrated. Gas viscosity reaches a large value because of high lamella concentration in this zone. For comparison purposes, we have added the global gas mobility reduction factor (FF) described in equation (12) to compute how much gas mobility is reduced with respect to a base case where no blocking effect is considered, i.e. blocking foam is not formed.

According to these results, the global gas mobility reduction factor can go from 250 at critical lamella molar fraction at the bottom foam zone to 2.5E+04 at maximum lamella molar fraction (0.1) at the uppermost zone of thief zone invaded by foam.

Figure 6 shows some profiles comparing the best performance obtained injecting steam alone, steam-gas co-

injection and foam injection in a second injector well for three and eight years after starting steam injection.

For the SAGD case, steam contacts fast the thief zone which causes an increment in temperature. After contacting the water zone, pressure communication occurs between the injector well and the thief zone and lateral expansion of the steam chamber is severely affected. Steam creates a communication path between the thief zone and the injector well where no too much fresh oil is contacted by steam. As shown in the figure after eight years of steam injection, temperature increases laterally at a higher velocity in the thief zone than in the pay zone.

Steam-gas co-injection results show that gas acts as an insulator between the steam chamber and the thief zone for some years. At some point between three and eight years of gas co-injection the steam chamber eventually contacts the thief zone. NCG is no longer able to delay contact of both fluids and steam invades the thief zone. No reduction in gas mobility is evidenced. Note that NCG co-injection with steam alters the steam chamber shape, forcing the lateral expansion that is not detected for the case where only steam is injected.

For the foam injection strategy, formed foam is able to invade the reservoir top and the thief zone. It seems that foam is not only able to isolate steam and water but also to displace water present in the thief zone. Due to its blocking ability quantified by the global gas mobility factor, steam is forced to expand laterally contacting more fresh oil and contacting eventually the thief zone if foam expansion velocity in the horizontal direction is not large enough. According to Figure 6, foam injection causes steam chamber expansion more to right side in the pay zone than any other strategy.

Figure 7 to Figure 12 compare results for the selected cases during fifteen years of SAGD operation. In general, the SAGD stepped decline case requires injecting more water to produce the worst results in term of recovery factor, cumulative steam-oil ratio and fraction of heat retained in the pay zone. Gas co-injection and foam injection produce interesting results that should analyzed in detail. Gas co-injection is able to generate better performance than foam in a second injector well during the first seven years of steam injection. After that, the steam chamber enters in contact with thief zone (2700 days), instantaneous steam-oil ratio increases sharply and large amounts of heat are transferred to the water zone. Only 10 percentage of additional oil is recovered once NCG-steam chamber enters into the top water zone. On the contrary, foam injection acts in a way that produces more stable results. No major changes are evidenced in the trend described when foam is injected during this period. As a result, oil recovery can reach 50% OOIP without no sharply heat losses to the thief zone and a very low instantaneous steam-oil ratio after fifteen years of foam injection.

Table 6 and Table 7 summarized comparative results after ten and fifteen years of numerical simulation. Larger simulation times (15 years) were required to show favorable effects of foam injection respect with gas co-injection. Table 6 is shown only for comparative purposes with previous summarized tables. According to Table 7, foam injection requires 33 percentage less water and 50 percentage less NCG than best performance during gas co-injection strategy.

Recovery factor and CSOR are 52% and 3.0, respectively, when foam is injected. Heating rate exchange between steam and water in the thief zone is larger for the gas co-injection case than it is for the foam injection strategy. When foam is injected at the reservoir top, 30% of the total heat injected during fifteen years is retained in the pay zone while only 20% of the total heat is retained when NCG is co-injected. According to these results, foam injection requires less water and gas than gas co-injection, and less water than optimal strategy for the SAGD base line case. As a conclusion, the highest value of oil recovery, the lowest value of cumulative steam oil ratio and the largest percentage of heat accumulated in the pay zone with respect to total heat injected were found for the foam injection strategy with a second foam injector on top.

3.4 Effect of gas mobility reduction

Figure 13 shows profiles of lamella molar fraction in the gas phase, gas mobility reduction factor and steam chamber temperature for different levels of foam blockage. Blocking factors were defined by equation (12) at critical lamella molar fraction in the gas phase. Values defined in this form permit to obtain a minimum blockage factor in presence of foam. Gas mobility reduction factors (FF) between 2500 and 1 were studied in this work. The foam base case discussed above had a FF=250. Figure 13 shows no blocking effect for the case where a foamer was not injected (FF=1). For a high level of gas mobility reduction (FF=2500 and 1250), lamella concentration limits its action to around the injector well without no major effective blockage in the thief zone. The high level of local blockage around the injector well causes the injection pressure to reach faster its maximum pressure constraint with only a reduced volume of chemical treatment. On the contrary, effective foam propagation was obtained for intermediate blocking level, i.e., 250 and 25. Optimal results were obtained for FF=25 due to foam occupied volume. This behavior is promoted by large injected gas volume *and* a convenient level of effective gas mobility reduction factor. Values of injected gas required to form foam are shown in Table 8. Values of injected gas were inversely proportional to the specified global gas mobility reduction factor. Gas volume injected for Case FF=1 shows that only a large volume of injected gas is not enough to isolate effectively steam chamber and water cap. Case FF=25 shows that is also necessary to reduce the gas mobility in at least three order of magnitude (horizontal and vertical permeability are 1000 and 600 mD, respectively) to improve thermal efficiency of the SAGD process. This case permits to obtain the largest value of heat accumulated in the pay zone, the largest recovery factor, and the minimum CSOR.

3.5 Effect of oil saturation in foam decay rate

The effect of initial oil saturation on foam decay is shown in Figure 14 after five years of steam injection. For case $So_{initial}=0$, oil was not initially present in the thief zone while for the other case, an initial oil saturation of 20% was specified. This figure shows that some oil fraction is displaced to the thief zone due to the vertical steam chamber growth. In addition, residual oil saturation present around the foam injector can alter foam stability. Figure 14 shows that

foam performance is highly altered when oil effect is taken into account. The foam chamber size is not large enough to prevent thief zone contact between water and steam. If these cases are compared to the foam base case where no foam decay is considered (Figure 5), foam chamber is reduced in size and in ability to reduce gas mobility. In the cases where weaker foam is formed (So=0 and foam decay), steam divers foam and contacts the thief zone. The reason that explains this behavior is that foam decay reduces lamella concentration in the gas phase which is not high enough to reduce gas mobility in the thief zone.

Table 9 summarizes results for a foam case where no foam decay was specified and no oil was initially present in the reservoir top and cases where foam decay were considered in presence of oil. Comparison of results shows that steam chamber size can be 30 percent smaller in volume when foam decay is taken into account and even much smaller (40%) if initial oil saturation equals 0.20 in the thief zone. According to these simulation results, foam degradation by oil can play an important role in the ability of foam to improve thermal efficiency of SAGD process with a thief zone located above it. However, we do not discard the existence of foam formulation (surfactants and additives) able to form strong foam at low oil saturations (So< 0.20).

3.6 Final comments

Simulations results show that foam formation on top of the reservoir is able to control heat losses to the thief zone. This implies the application of chemical products with a dedicated well in a region close to the thief zone and low oil saturation. One of major challenges in a chemical injection is to place correctly the product in the desired zone that could be highly heterogeneous and to assure the thermal and chemical stability of the blocking agent. Recently some authors (Emadi *et al*, 2011) have published experimental results using foam in micro-models to displace mobile heavy oils at reservoir temperature. They showed that a non-condensable gas, N2 as a foamer, forms very stable foam even in presence of high values of oil saturation. It is unknown if their formulation will also be stable at steam injection conditions.

On the other side, Schramm and Novasad (1992) have suggested that foam decay can depend on oil composition. They found that light fractions are most destabilizing to foam than heavy oil fractions. Oil composition effect has not well been studied for heavy oils. This requires an experimental effort in order to identify oil components and oil groups that tend to break up foam lamellae.

Concerning to the simulation model, we think that our foam model can be improved, for instance, considering a permeability reduction function which depends on lamella adsorption on rock. The inclusion of this modification in the model implies that adsorption data at different temperatures should be known.

Finally, it is necessary to point out that results shown in this paper are based on different data reported in literature. A large numbers of parameters for describing the generation of foam based on the assumption of non-equilibrium were necessary. Taking into account that these parameters are highly dependent on the chemical formulation and the application conditions in the reservoir, experiments should be done in order to measure them or to obtain them by history matching. The identification of surfactant able to generate

stable foams at steam injection conditions in a heavy oil reservoir is also a major task that might be accomplished in the near future.

4 Conclusions

- Steam injection strategies during a SAGD process in presence of thief zone with low values of steam-oil ratio implies injection pressure reduction before the steam chamber contacts the thief zone. If steam crosses the reservoir top, pressure communication with the thief zone occurs and most of steam latent heat is lost to the water cap.
- An optimal steam injection strategy for treating a heavy oil reservoir submitted to a SAGD process with a thief zone above it requires low steam injection pressures and low water volumes which imply large exploitation periods.
- Gas co-injection can retard contact between injected steam and fluid presents in the thief zone if the gas cap is thickness enough. Once gas enters the thief zone no more insulating effect exists and thermal efficiency is severely affected.
- Foam injection strategy can improve thermal efficiency in presence of a thief zone. Simulation results show that foam is not only able to isolate steam and water but also to displace water present in the thief zone. Due to its blocking ability the steam chamber is forced to expand laterally producing the largest value of oil recovery and the lowest value of steam-oil ratio.
- Result for gas injection in a second horizontal well without gas mobility reduction show that injecting only gas is not enough to isolate effectively the steam chamber and the water cap.
- A foam formulation able to reduce gas mobility over (at least) three orders of magnitude accompanied by a large foam expansion on the reservoir top seems to be the best strategy to limit vertical expansion of the steam chamber.
- When foam decay by presence of oil is considered in the model, foam performance results in weaker foam which affects severely thermal efficiency of the process.

Acknowledgement

Nomenclature

$Y_{l(gas)}=$	molar fraction of lamella in the gas phase
$\mu_g^o =$	original viscosity of the gas phase, cP
$\mu_l =$	lamella effective viscosity, cP
$RRF =$	residual resistance factor for adsorbed lamellae
$Ad_l=$	current lamella adsorption conc., $gmol/m^3$
$Al_{max} =$	maximum adsorption capacity, $gmol/m^3$
$r_{lg/c/d}=$	lamella generation/coalescence/decay, gmol/day
$r_{Lamella}=$	lamella degradation, gmol/day
$q_l=$	source/sink term for lamella
$\vec{u}_g=$	gas velocity
$Y_l=$	molar fraction in gas phase
$\varphi=$	porosity
$S=$	phase saturation
$\rho_\beta=$	beta phase molar density
$FM=$	gas resistance factor
$K_{rg}=$	gas relative permeability
$K_{rg}=$	gas relative permeability
$\lambda_g =$	gas mobility
$K=$	absolute permeability, mD
$\mu_g=$	gas phase viscosity, cP
$K_i=$	constant velocity for reaction i
$A_i=$	pre-exponential factor for reaction i
$E_{ai}=$	activation energy, kJ/gmol
$T=$	absolute temperature, K
$R=$	ideal gas constant
$C_{i\beta}=$	concentration of comp I in phase β, $gmol/m^3$
$FF=$	global gas mobility reduction factor, ad

Super-indices

$_o=$	standard, foam is not present
$_{foam}=$	foam is present

Sub-indices

$\beta=$	phase (oil, gas, aqueous)
$Surf=$	surfactant
NCG=	non-condensable gas

References

1. Alturki, A., Gates, I.D., Maini, B., "On SAGD in oil sands reservoirs with no cap rock", SPE paper 137234, paper presented at the Unconventional Resources and International Petroleum Conference held in Calgary, 19-21 October, 2010.

2. Bao X., Chen Y., Wie, Y., Sun C.C., Dong, Deng. H., and Song., Y., "Geostatistical modeling and numerical simulation of the SAGD process: case study of an

Athabasca reservoir with top water and gas thief zones", SPE paper 137435, presented at the Canadian Unconventional Resources & international Petroleum Conference held in Calgary, 19-21 Octobre 2010.

3. Butler, R., "The steam and gas push (SAGP)" Journal of Canadian Petroleum Technology, Vol. 38, number 3, pp. 54-61, 1999.

4. Butler, R., "The behavior of non-condensable gas in SAGD – a rationalization", Journal of Canadian Petroleum Technology, Vol. 43, number 1, 2004.

5. Chen, Q., Gerritsen, MG., Kovscek, AR. "Improving steam-assisted gravity drainage using mobility control foams: foam assisted-SAGD, FA-SAGD", SPE paper number 129847, paper presented at the SPE Improved Oil Recovery Symposium held in Tulsa, OK, 24-28-April 2010.

6. Chen, Q., Gerritsen, MG., Kovscek, AR. "Modeling foam displacement with the local-equilibrium approximation: theory and experimental verification", SPE paper number 116735, SPE Journal, Vol 15, number 1, March 2010.

7. Chen, Q., PhD dissertation, Assessing and improving steam-assisted gravity drainage: reservoir heterogeneities hydraulic fractures and mobility control foams, May, 2009.

8. Chou, SI., "Conditions for generating foam in porous media", SPE paper number 22628 presented at the Annual technical Conference and Exhibition, Dallas, TX, 1995.

9. Coombe, D.A., Oballa, V., and Buchanan, W.L., "Foam modelling based on lamella as dispersed component," CMG Technical Report 90.08.T, April 1990.

10. Emadi, A., Sohrabi, M., Jami, M., and Robertson G., "Visual investigation of extra-heavy oil recovery by CO2/N2 foam injection", paper A23 presented in the 16th EAGE IOR 2011.

11. Fisher A., Foulser R., and Goodyear S., "Mathematical modeling of foam flooding", paper SPE number 20195 presented at the SPE /DOE Enhanced Oil Recovery Symposium, Tulsa, OK, April 22-25,1990.

12. Friedmann F., and Jensen, J.A. "Physical and chemical effect of an oil phase on the propagation of foam in a porous media". SPE paper number 16375, presented at the SPE California Regional meeting, held in Ventura, California, 6-8 Apr, 1987.

13. Friedmann F., Chen, W.H., Gauglitz P.A. "Experimental and simulation study of high-temperature foam displacement in porous media." SPE Reservoir Engineering paper number 17357, February 1991.

14. Gates, I. D. and Chakrabarty, N., "Optimization of steam assited gravity drainage in McMurray Reservoir", JCPT, September 2006, Vol 45, number 9.

15. Gates, I.A., Kenny J., Hernandez-Hdez, I. and Bunio, G.,"Steam-injection strategy and energetics of steam-assisted gravity drainage", SPE Reservoir Evaluation & Engineering, SPE number 97742, February 2007.

16. Hirasaki, G., "The steam foam process", JPT May 1989.

17. Islam, MR, Farouq Ali, SM, " Numerical simulation of foam flow in porous media", Journal of Canadian Petroleum Technology, July-August 1990, Vol. 29, number 4.

18. Ito Y., Ichikawa, M. and Hirata, T. "The effects of gas injection on oil recovery during SAGD projects" Journal of Canadian Petroleum Technology, Vol. 40, number 1, 2001.

19. Ito Y., Ichikawa, M. and Hirata, T. "The effects of gas injection on oil recovery during SAGD projects" Journal of Canadian Petroleum Technology, Vol. 40, number 1, 2001.

20. Kovscek AR., Patzek, TW., Radke CJ., "Mechanistic prediction of foam displacement in multidimensions: a population balance approach", SPE paper number 27789, presented in the nineth symposium on improved oil recovery held in Tulsa, OK, 17-20 April 1994.

21. Lau E.C., and Coombe, D.A., "History matching the steam/foam injection process in a thick Athabasca tar sand reservoir", JCPT , Vol 33, number 1, 1994.

22. Law, D.H. and Nasr T.N., Beaulieu, G., Golbeck, H., Korpany, G., "SAGD application in gas cap and top water oil reservoirs", paper presented at the Petroleum Society's Canadian International Petroleum Conference, Calgary, paper number 2000-20, June 4-8, 2000a.

23. Law, D.H. and Nasr T.N., "Lab-scale numerical simulation of SAGD process in the presence of top thief zones: a mechanistic study", paper presented at the Petroleum Society's Canadian International Petroleum

Conference, Calgary, paper number 2000-21, June 4-8, 2000b.

24. Law H., Tawfik, Nasr, William Good,"Field-scale numerical simulation of SAGD process with top-water thief zone", SPE paper number 65522, 2000c.

25. Marfoe CH, Kazemi, H., "Numerical simulation of foam flow in porous media", SPE paper number 16790 presented at the 1987 Annual Technical Conference and Exhibition, Dallas TX, 27-30.

26. Nguyen Q., Alexandrov A., Pacelli Z., Currie P., "Experimental and modeling studies of foam in porous media : a review", SPE paper number 58799, presented at the SPE International Symposium on Formation Damage Control, held in Lafayette, Louisiana, 23-24 Feb, 2000.

27. Patzek, T., "Field application of steam foam for mobility improvement and profile control", SPE reservoir engineering, SPE number 29612, May 1996.

28. Rossen W., Gauglitz, P., "Percolation theory of creation and mobilization of foam in porous media", Am. Inst. Chem. Eng. Journal, 1990, Vol 36, pag. 1176.

29. Rossen W., Zhou Z., and Buchanan L., "Modeling foam mobility in porous media", Paper SPE number 22627 presented at the 66th Annual technical Conference, Dallas, TX, 1991.

30. Sander P., Clark G., Lau E.,"Steam-foam diversion process developed to overcome steam override in Athabasca", SPE paper number 22630, presented at the 66th annual technical conference and exhibition of the SPE held in Dallas, Texas, October 6-9, 1991.

31. Schramm, L., and Novasad, J., "The Destabilization of Foams for Improved Oil Recovery by Crude Oils: Effect of the Nature of the Oil." Journal of Petroleum Science & Engineering vol. 7(No. 1-2): 77-90 Elsevier Science, 1992.

32. STARS Manual, 2011a. CMG templates. Lamella model for foam generation in a core. stdrm011.dat.

33. STARS Manual, 2011b. CMG templates. Lamella model for foam generation with oil. stdrm013.dat.

Table 1 Components and phase distribution for the foam model.

Components/Phases	Aqueous (aq)	Oleic (o)	Gaseous (g)	Adsorbed (s)
Water (18)	X		X	
Oil (500)		X		
CH4 or NCG (16)			X	
Surfactant (480)	X			X
Lamella (18)			X	

Table 2. Kinetic parameters for some pseudo-reactions in foam model

Reactions	Pre-exponential factor,	Activation energy, kJ/gmole
Lamella generation	$300\left[\left(\dfrac{gmole}{m^3}\right)^{-1}\cdot\dfrac{1}{day}\right]$	-
Lamella coaslescence	$2477\left[\left(\dfrac{gmole}{m^3}\right)^{-1}\cdot\dfrac{1}{day}\right]$	-
Surfactant degradation	$34.7\left[\dfrac{1}{day}\right]$	32.5
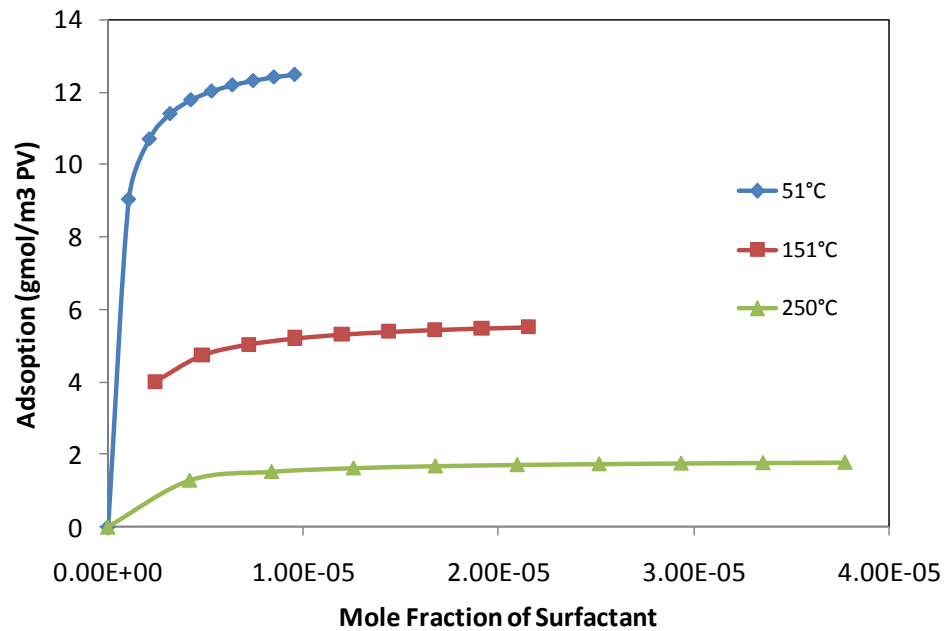
Figure 1. Adsorption of surfactant as a function of temperature and concentration of surfactant in water phase.
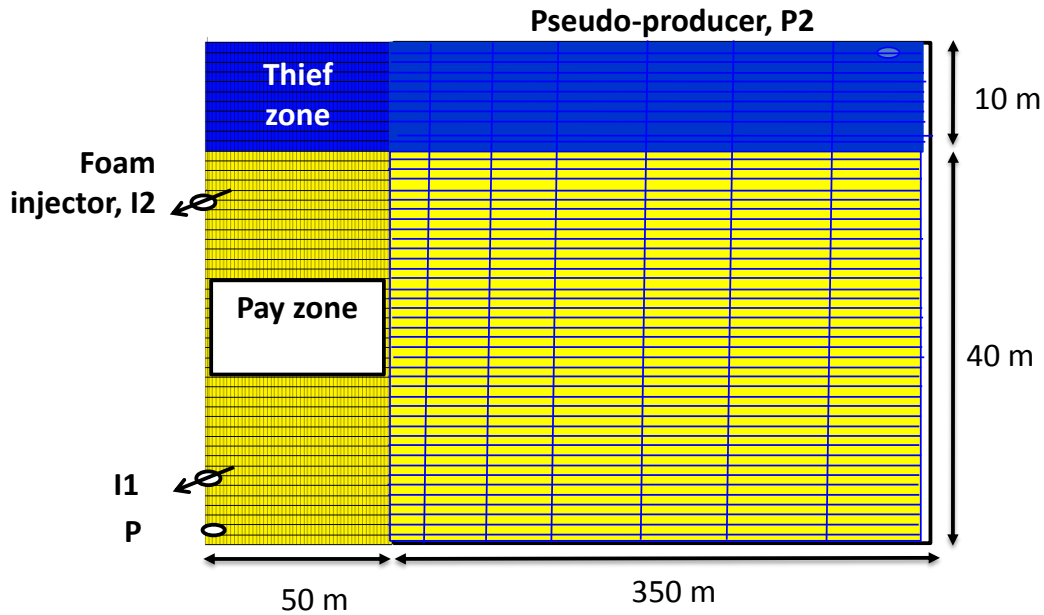
Figure 2. Reservoir model description.

Table 3. Reservoir properties.

Properties	
Reservoir depth (top of pay zone)	300 m
Reservoir depth (top of thief zone)	290 m
Initial reservoir pressure at 300 m	1000 kPa
Thickness (pay zone – thief zone)	40 - 10 m
Porosity (pay zone – thief zone)	0.3 - 0.2
Horizontal permeability (pay zone – thief zone)	2000 -1000 mD
Vertical permeability (pay zone – thief zone)	1200 – 600 mD
Oil viscosity at 50°C	8028 cP
Initial temperature	10°C
Initial oil saturation (pay zone –thief zone)	0.8 – 0.0
Initial water saturation (pay zone- thief zone)	0.2 – 1.0
Oil gravity	8 API

Table 4. Summary results for SAGD cases after ten years of numerical simulation.

	Cumulative injected steam, 10^6 m^3 of CWE	Cumulative steam-oil ratio, m^3/m^3	Recovery factor, % OOIP	Percentage of heat accumulated in the pay zone to total heat injected, J/J
Overbalance	1.29	11.6	26.6	14.9
Under Balance	0.71	7.5	22.7	21.7
Stepped decline	0.69	7.4	22.2	21.7
SOR control	0.69	7.4	22.0	21.7

(a)   (b)
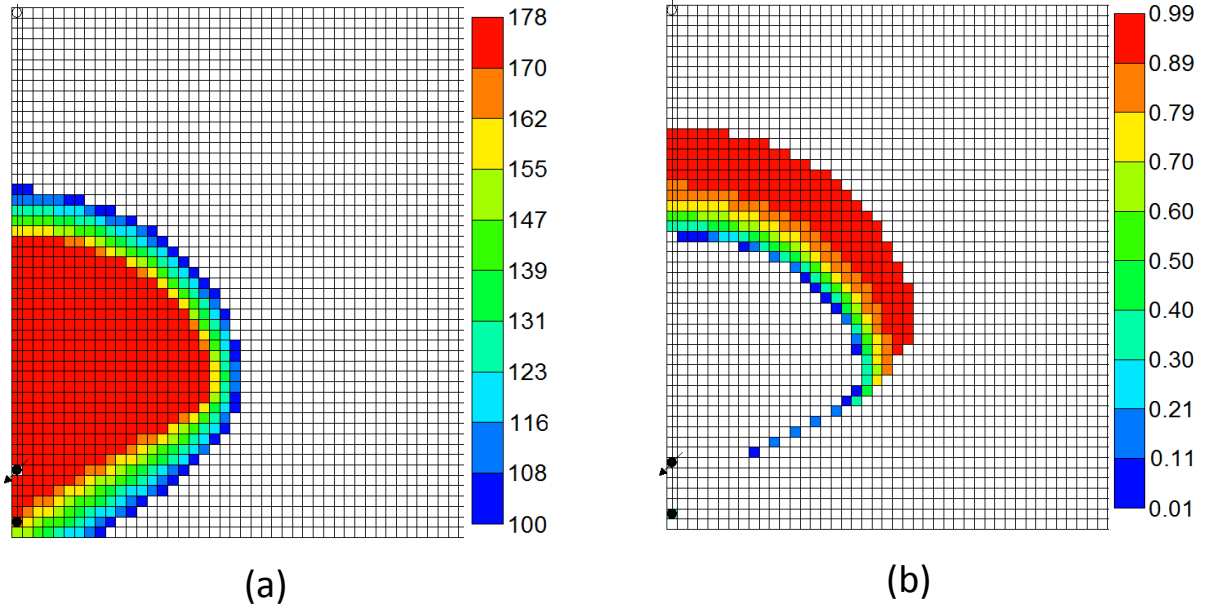
Figure 3. (a) Steam chamber temperature (°C) and (b) NCG molar fraction in gas phase after five years of simulation.

Table 5. Summary results for NCG co-injection with steam in SAGD injector after ten years of simulation (50% volume of NCG injected)

	Cumulative injected steam, 10⁶ m³ of CWE	Cumulative injected gas, 10⁶ m³ at SC	Cumulative steam-oil ratio, m³/m³	Recovery factor, % OOIP	Percentage of heat accumulated in the pay zone to total heat injected, J/J
Over balance	1.28	1.19	11.3	27.2	15.0
Under balance	0.66	0.57	6.9	22.8	22.1
Stepped decline	0.54	0.49	4.4	29.7	28.4
SOR control	0.62	0.54	6.9	21.8	22.5

NCG molar fraction in gas phase

Ternary diagram

NCG co-injection managing injection pressure with SOR control

NCG co-injection stepped declining strategy
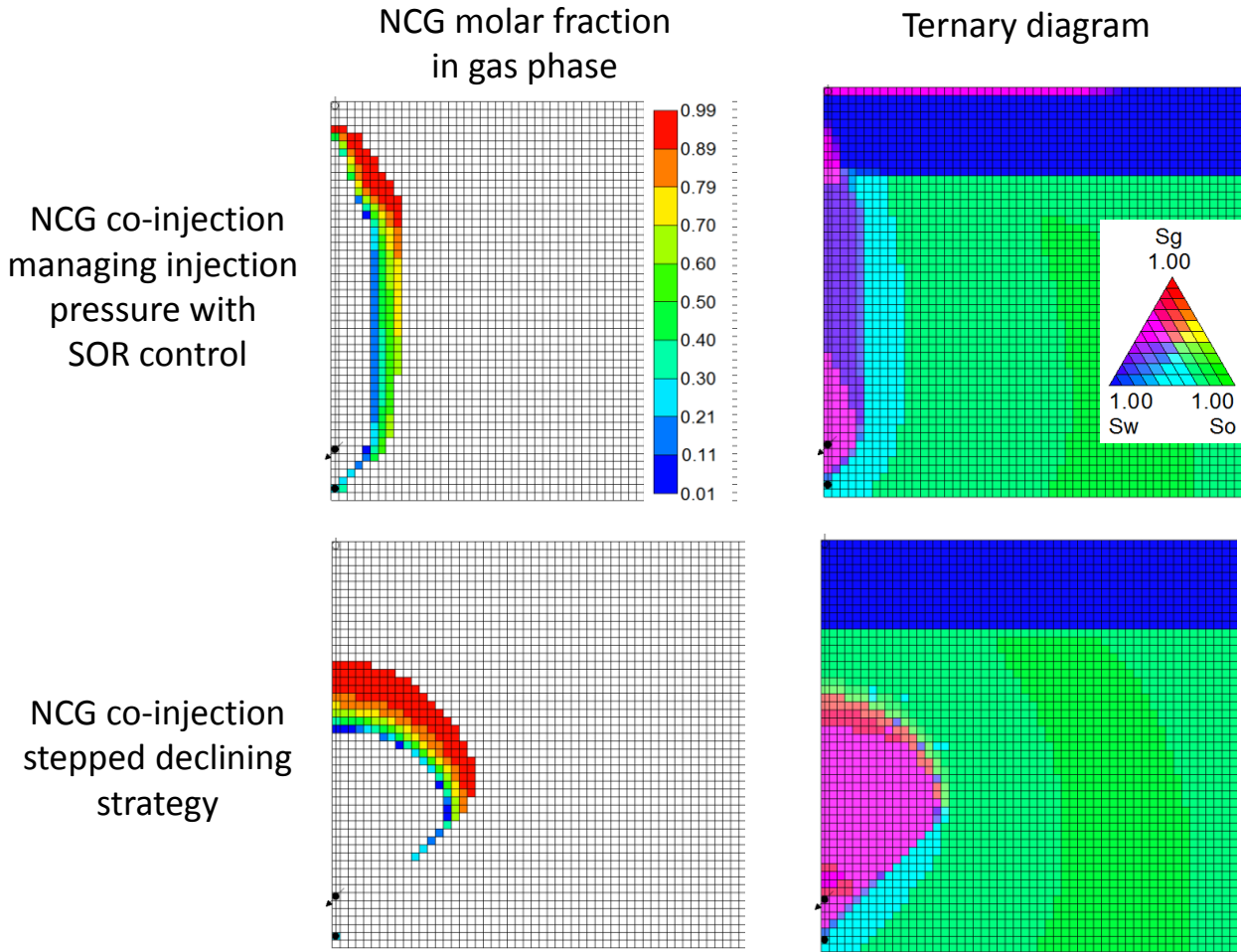
Figure 4. Comparison of NCG molar fraction in gas phase and ternary diagram after three years of simulation for two different NCG co-injection strategies in SAGD well.

Lamella gas mole fraction

Gas relative permeability

Gas viscosity, cP

Global gas mobility reduction factor
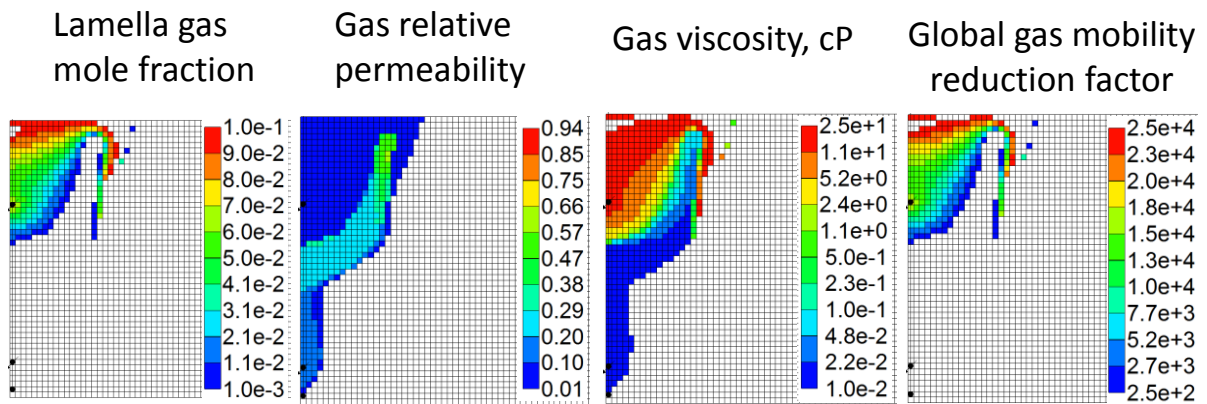
Figure 5. Some properties profiles for foam injection strategy at the reservoir top after five years of steam injection in SAGD pair.
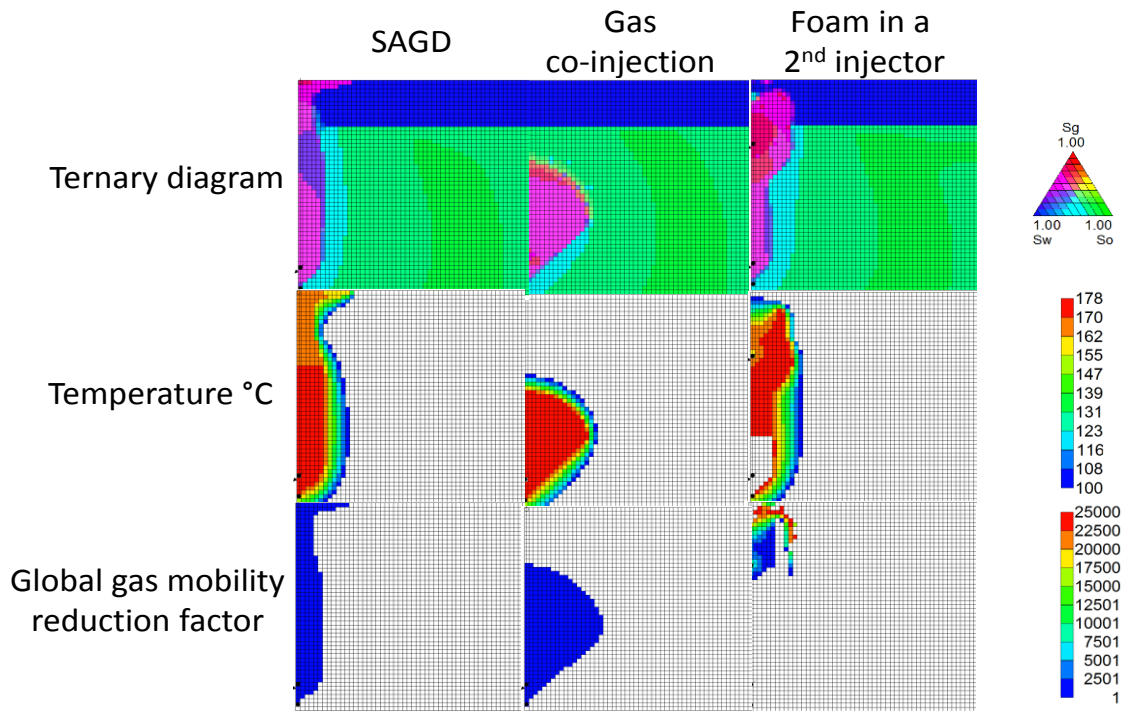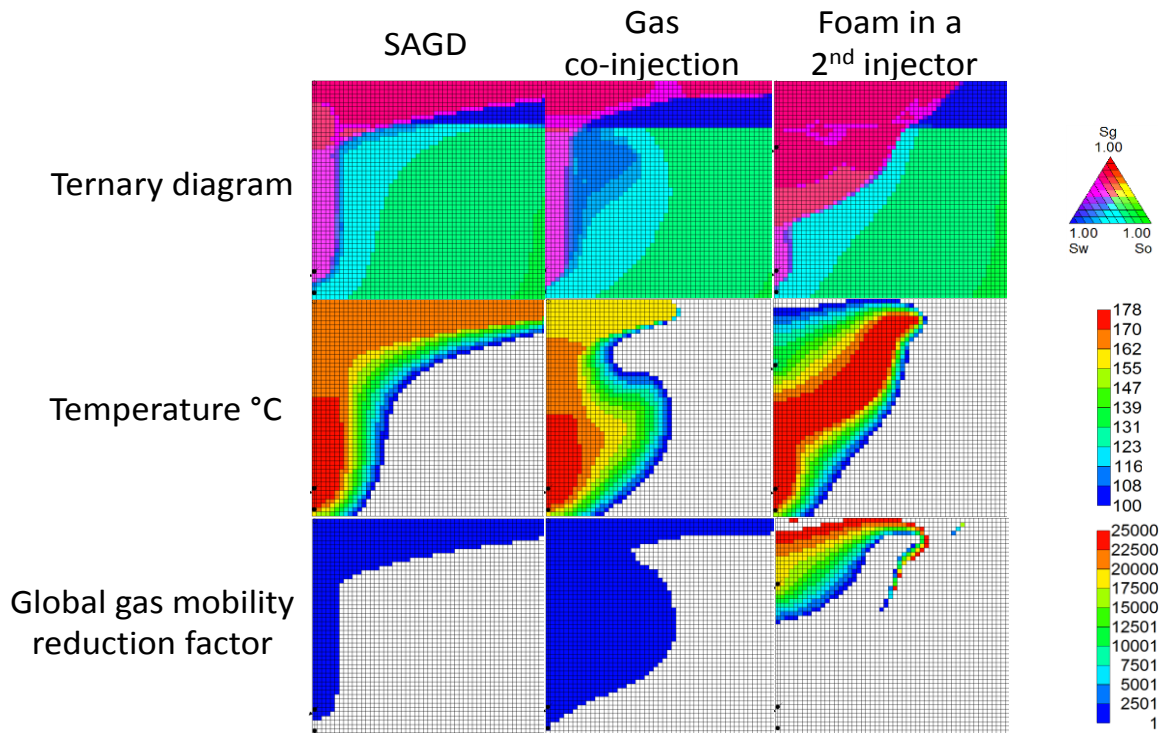
Figure 6. Some property profiles after (a) three years and (b) eight years of simulation for three different cases: stepped decline SAGD, stepped decline NCG co-injection in SAGD well and foam injection at the reservoir top with a SAGD pair.
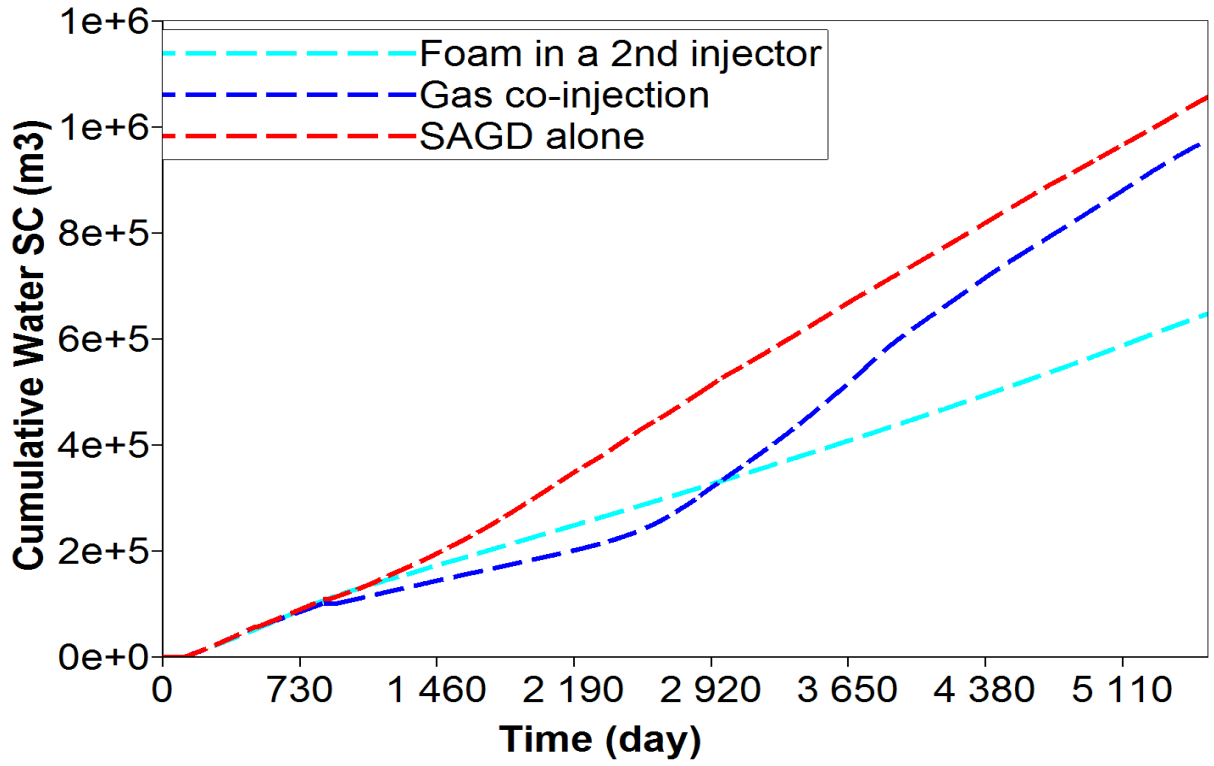
Figure 7. Accumulated steam injection.
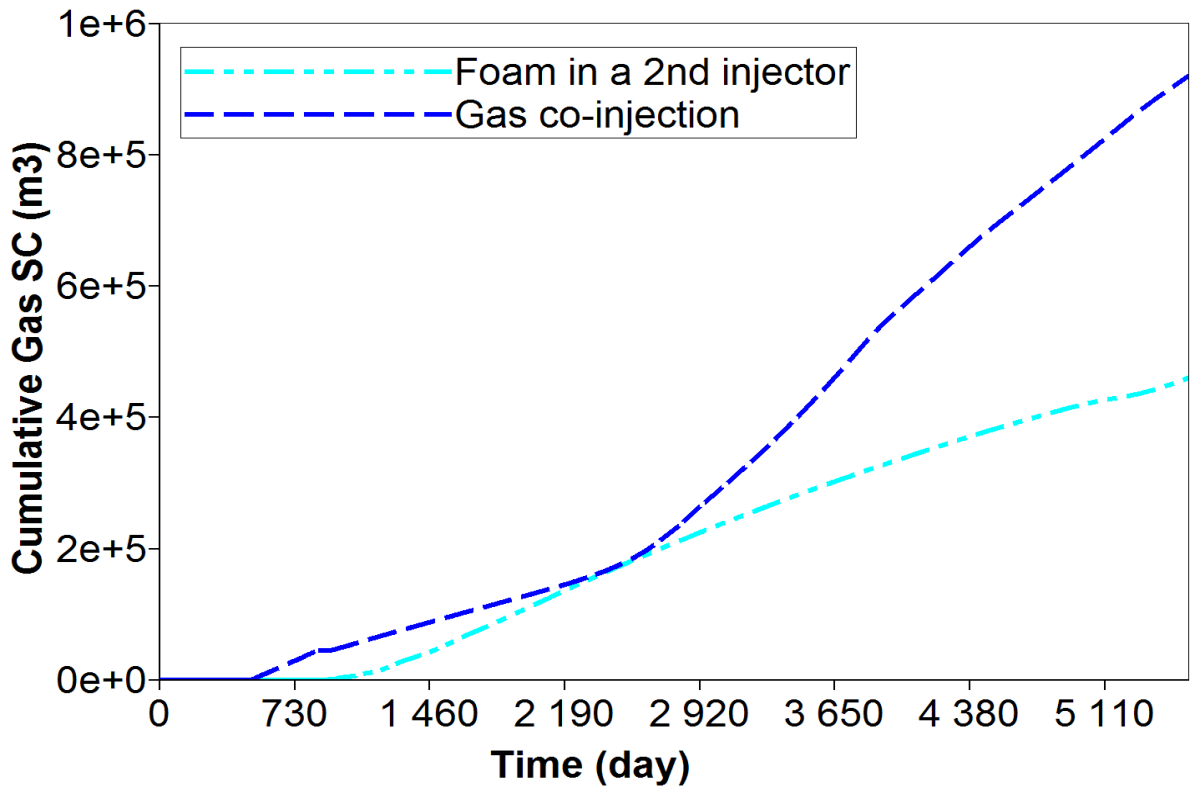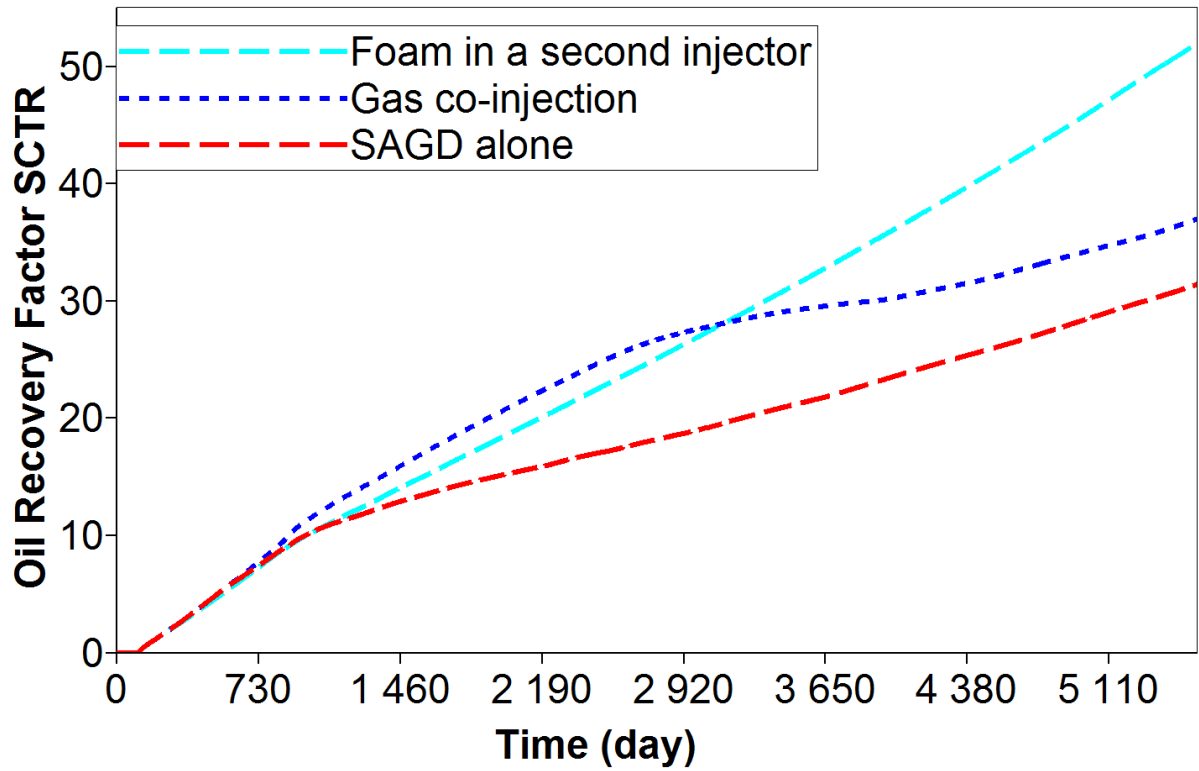

Figure 8. Cumulative gas injected.
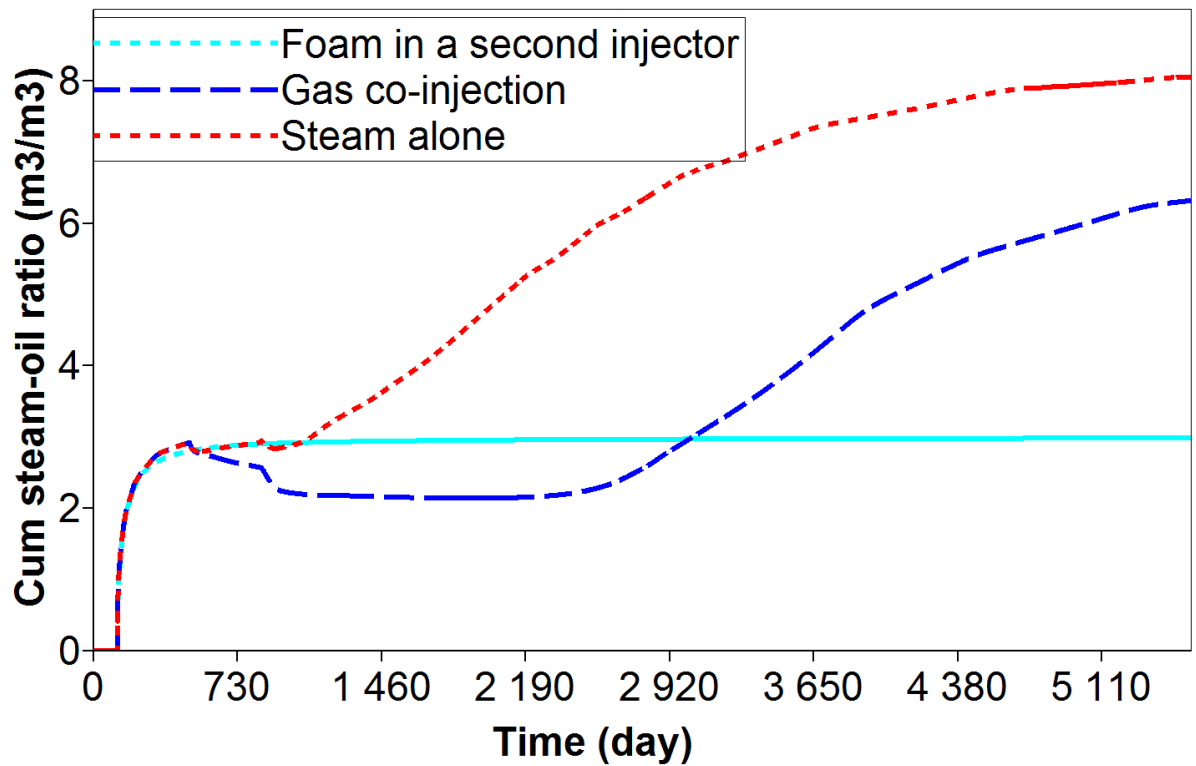
Figure 9. Comparison of oil recovery factor.
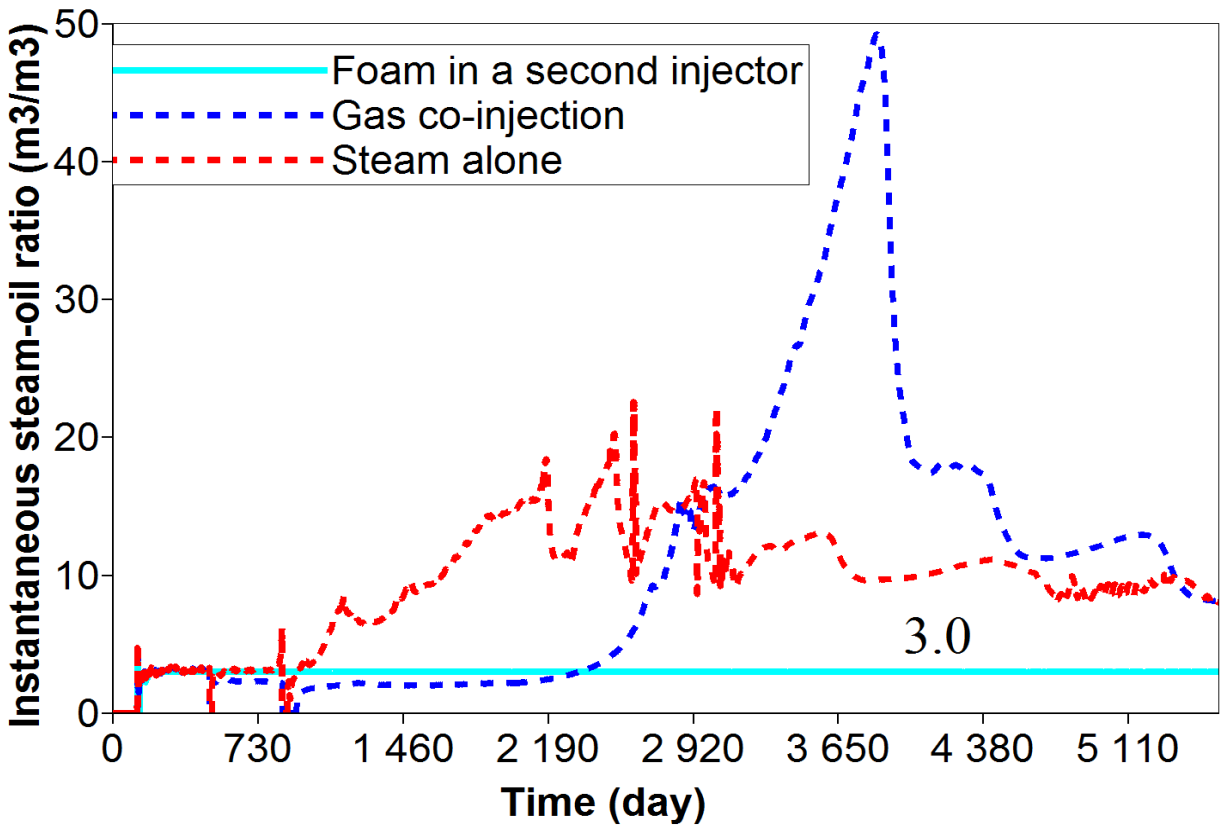

Figure 10. Comparison of cumulative steam-oil ratio.

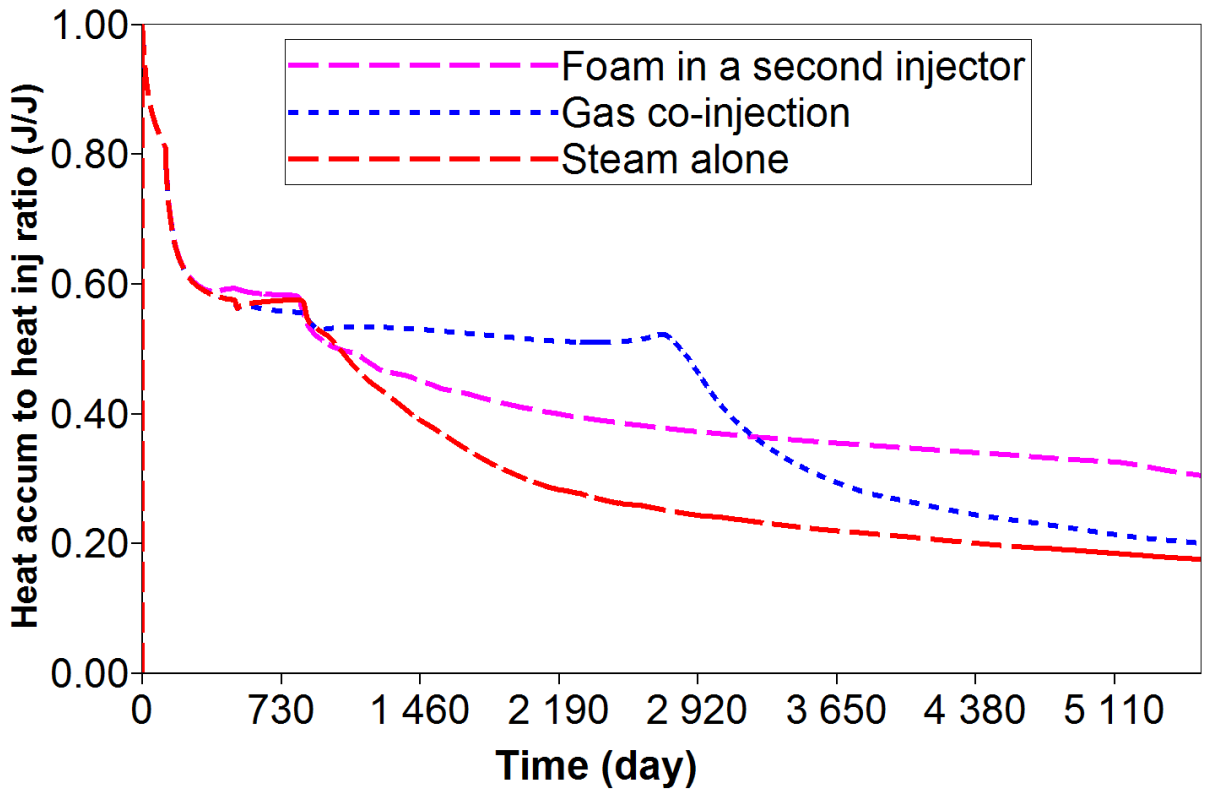**Figure 11. Comparison of instantaneous steam-oil ratio.**

Figure 12. Comparison of heat acummmulated in the pay zone with respect to total injected heat.

Table 6. Summary of best results for steam alone strategy, gas co-injection in SAGD well and foam injection on reservoir top after ten years of simulation

	Cumulative injected steam, 10^6 m^3 of CWE	Cumulative injected gas, 10^6 m^3 at SC	Cumulative steam-oil ratio, m^3/m^3	Recovery factor, % OOIP	Percentage of heat accumulated in the pay zone to total heat injected, J/J
SAGD base line case	0.69	0.00	7.4	22.2	21.7
Gas co-injection	0.54	0.49	4.4	29.7	28.4
Foam in a second injector	0.42	0.31	3.0	33.7	35.8

Table 7. Summary of best results for steam alone strategy, gas co-injection in SAGD well and foam injection on reservoir top after fifteen years of simulation

	Cumulative injected steam, 10^6 m^3 of CWE	Cumulative injected gas, 10^6 m^3 at SC	Cumulative steam-oil ratio, m^3/m^3	Recovery factor, % OOIP	Percentage of heat accumulated in the pay zone to total heat injected, J/J
SAGD base line case	1.06	0.00	8.1	31.4	17.5
Gas co-injection	0.98	0.92	6.3	37.0	20.0
Foam in a second injector	0.65	0.46	3.0	51.9	30.5

Table 8. Summary of results for different levels of global gas mobility reduction factor after ten years of simulation.

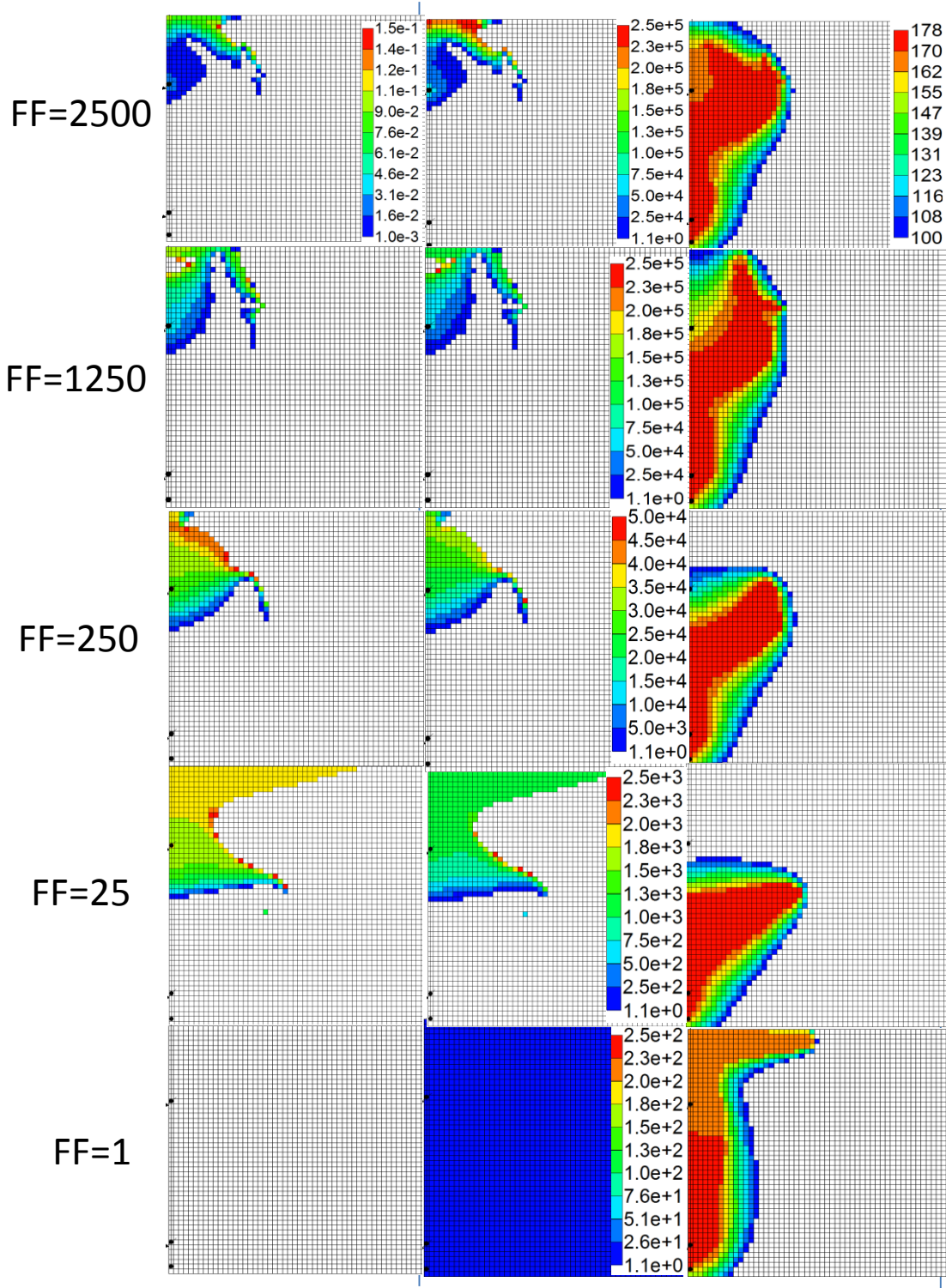| Global gas mobility reduction factor, FF	Injected gas volume, 10^6 m^3 SC	Cumulative steam-oil ratio, m^3/m^3	Recovery factor, % OOIP	Percentage of heat accumulated in the pay zone to total heat injected, J/J
2500	0.08	3.5	32.2	33.1
1250	0.13	3.4	32.6	33.1
250	0.31	3.0	33.7	35.8
25	0.83	2.5	39.0	44.0
1	1.13	6.7	22.4	23.2

Figure 13. Some property profiles for different blocking levels (FF) in presence of foam after five years of steam injection in SAGD pair.
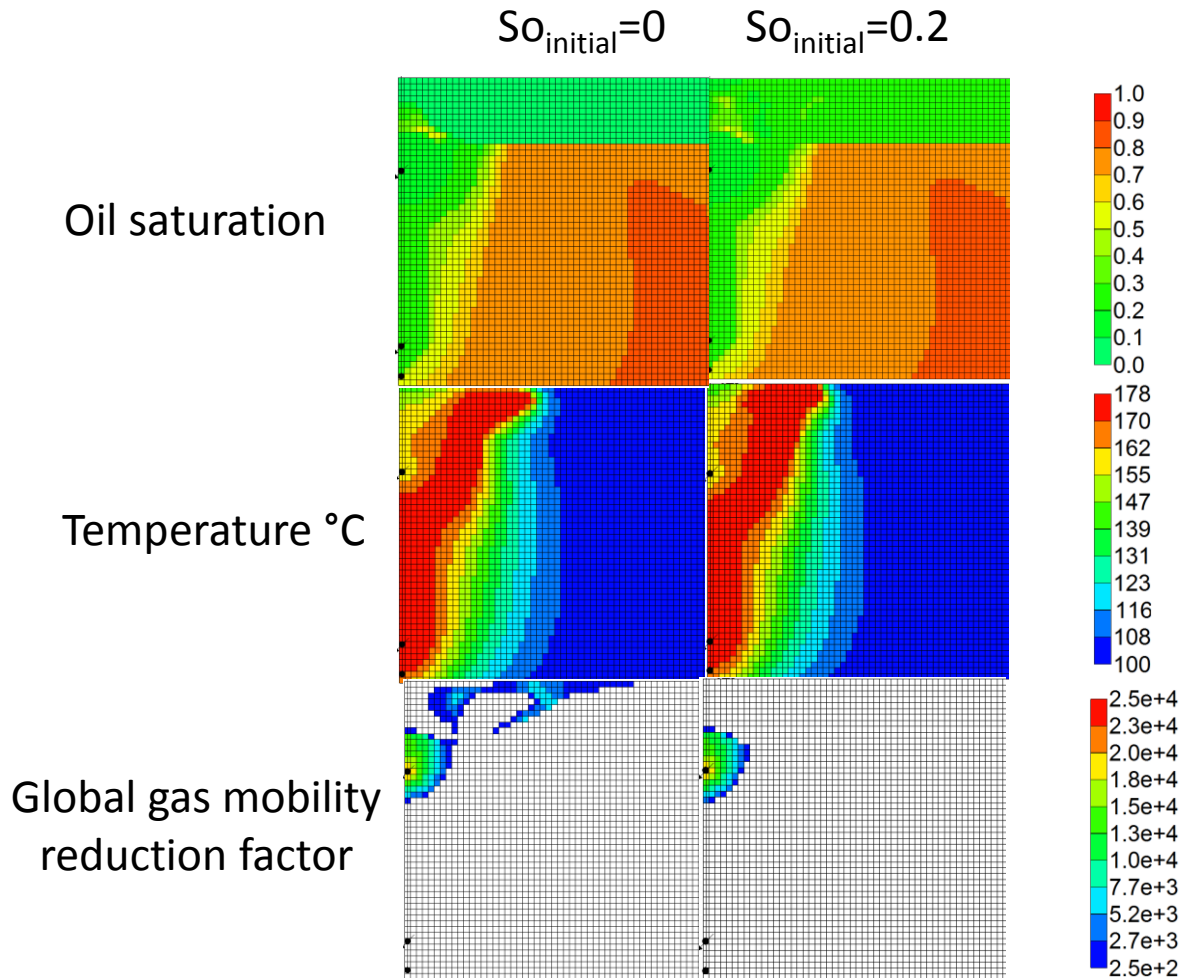
Figure 14. Some property profiles during foam treatment in the second injector well taken into account the effect of oil saturation in foam decay after 5 years of simulation.

Table 9. Effects of oil saturation on foam performance after ten years of simulation.

Initial oil saturation in thief zone, S_o	Steam chamber volume, 10^4 m³ SC	Cumulative steam-oil ratio, m³/m³	Recovery factor, % OOIP	Percentage of heat accumulated in the pay zone to total heat injected, J/J
0 & no foam decay	8.4	3.0	33.7	35.8
0 & foam decay	5.5	4.3	27.9	30.8
0.2 & foam decay	4.8	4.8	26.7	27.0